



HHS Public Access

Author manuscript

J Am Chem Soc. Author manuscript; available in PMC 2018 March 15.

Published in final edited form as:

J Am Chem Soc. 2017 March 15; 139(10): 3736–3746. doi:10.1021/jacs.6b12654.

Asymmetric Alkylation of Anthrones, Enantioselective Total Synthesis of (–)- and (+)-Viridicatumtoxins B and Analogues Thereof: Absolute Configuration and Potent Antibacterial Agents

K. C. Nicolaou^{†,*}, Guodu Liu[†], Kathryn Beabout[‡], Megan D. McCurry[‡], and Yousif Shamoo[‡]

[†]Department of Chemistry, BioScience Research Collaborative, Rice University, 6100 Main Street, Houston, Texas 77005, United States

[‡]Department of Biochemistry and Cell Biology, Rice University, 6100 Main Street, Houston, Texas 77005, United States

Abstract

A phase transfer catalyzed asymmetric alkylation of anthrones with cyclic allylic bromides using quinidine- or quinine-derived catalysts is described. Utilizing mild basic conditions and as low as 0.5 mol % catalyst loading, and achieving up to >99:1 dr selectivity, this asymmetric reaction was successfully applied to produce enantioselectively (–)- and (+)-viridicatumtoxins B, and thus allowed assignment of the absolute configuration of this naturally occurring antibiotic. While the developed asymmetric synthesis of C10 substituted anthrones is anticipated to find wider applications in organic synthesis, its immediate application to the construction of a variety of designed enantiopure analogues of viridicatumtoxin B led to the discovery of highly potent, yet simpler analogues of the molecule. These studies are expected to facilitate drug discovery and development efforts toward new antibacterial agents.

Graphical abstract

*Corresponding Author: kcn@rice.edu.

Supporting Information

The Supporting Information is available free of charge on the ACS Publications website at DOI: 10.1021/jacs.6b12654.

Full experimental details and characterization data (PDF)

Crystallographic information file for compound **6a** (CIF)

Crystallographic information file for compound (–)-**11** (CIF)

Crystallographic information file for compound (+)-**11** (CIF)

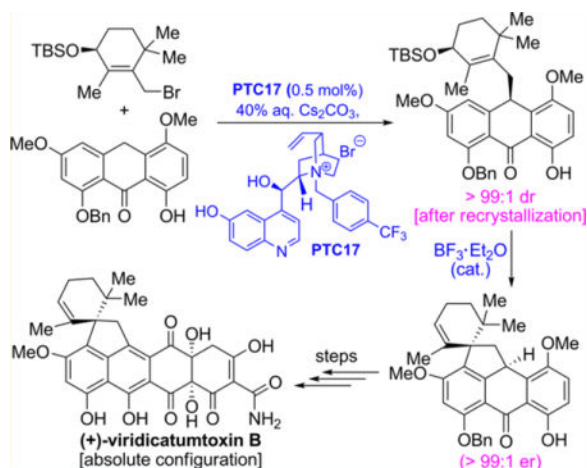
ORCID

K. C. Nicolaou: 0000-0001-5332-2511

Yousif Shamoo: 0000-0001-9241-8962

Notes

The authors declare no competing financial interest.



1. INTRODUCTION

The viridicatumtoxins [e.g., B (**1**)¹ and A (**2**)², Figure 1] and spirohexaline³ (**3**, originally reported structure, Figure 1) constitute a growing subgroup of the tetracycline class of naturally occurring antibiotics whose novel spirocyclic ring system (i.e., *EF* in **1a**) and high potencies against drug-resistant bacterial strains offer challenges and opportunities for synthetic chemists and microbiologists alike. Our recently reported total synthesis of viridicatumtoxin B (**1**) provided the natural substance in its racemic form and resulted in revision of its originally assigned structure (from **1a** to **1**, Figure 1).⁴ It also rendered readily available a number of less complex racemic analogues of viridicatumtoxin B that proved equipotent to the natural substance against methicillin-resistant *Staphylococcus aureus* (MRSA) and *Enterococcus faecium* strains.⁴ In view of the importance and recent emphasis on new antibacterial agents to combat dangerous bacterial infections, we sought to develop a general asymmetric synthesis of members of this family of compounds that includes, in addition to viridicatumtoxins B (**1**) and A (**2**)², spirohexaline (**3**, Figure 1).³ Interestingly, the latter compound was depicted in the original publication³ as shown in structure **3** despite its antipodal nature to that of its closest relative **2**, whose absolute configuration was determined by X-ray crystallographic analysis.⁵ This puzzling difference heightened the intrigue over the absolute configuration of viridicatumtoxin B (**1**).

2. RESULTS AND DISCUSSION

2.1. Asymmetric Alkylation of Anthrones

Figure 2 summarizes, in retrosynthetic format, the strategy employed in our first total synthesis of viridicatumtoxin B (**1**) in which the target molecule was traced back to key building blocks **5**, **7**, and **8** through advanced intermediates **4** and **6**, with the latter being the first key chiral compound enroute to **1**. The asymmetric generation of intermediate **6** through alkylation of anthrone **7** with cyclic allylic bromide **8**, therefore, became the key challenge for the sought-after asymmetric synthesis of viridicatumtoxin B and its analogues. This challenge was expected to be a thorny problem not only due to the potential propensity of alkylation product **6** to C10 (anthrone numbering) racemization under the required basic

conditions but also because of its perceived sensitivity to isomerize under the Lewis acid mediated spirocyclization conditions to form the next advanced intermediate, chiral pentacyclic compound **4** (viridicatumtoxin numbering). Although numerous asymmetric alkylations have been reported,^{6–11} a practical asymmetric alkylation of anthrones of type **7** was not available at the outset of this work.

Focusing on known asymmetric alkylation reactions,^{6–11} our initial studies pointed to phase transfer catalysts as promising for further studies. Brief exploration of phase transfer catalysts **PTC1** (Corey et al.)¹² and **PTC2** (Maruoka et al.)¹³ and chiral base catalyst **PTC3** (Hatakeyama et al.)¹⁴ identified the Corey catalyst (**PTC1**) as the most practical and efficient to pursue as a lead scaffold for further optimization (see Table 1, entries 1–3). Thus, following this pathpointing observation, we tested a series of catalysts (i.e., newly synthesized: **PTC5**, **PTC7–PTC13**, and **PTC15**; previously reported: **PTC4**,¹⁵ **PTC6**,¹⁶ **PTC14**,¹⁷ and **PTC16**,¹⁸ Table 1, entries 4–18; for further catalysts synthesized and tested, see Supporting Information) for their efficiency in the anthrone alkylation reaction with racemic [(*R,S*)-] or enantiopure [(*R*- or (*S*-)] allylic bromide **8** in a two-phase solvent system (50% aqueous KOH/CH₂Cl₂) at –78 to 0 °C. As seen in Table 1, the best results were obtained with **PTC15** and the (*R*)-enantiomer of allylic bromide **8** [(*R*)-**8**, 99% substrate conversion, 75% yield, 89:11 dr, entry 17], although the reaction with (*R,S*)-**8** also performed well (99% substrate conversion, 75% yield, and 86:14 dr, entry 15). The performance of **PTC9** and **PTC14** were also notable (entries 9 and 14, respectively, Table 1). The significant difference in diastereoselectivity observed with the (*S*)-enantiomer of **8** [(*S*)-**8**, entry 16, 83:17 dr] was noted with considerable interest. The ability to deliver the antipode of alkylation product **6** was demonstrated by using the (*S*)-enantiomer of allylic bromide **8** and catalyst **PTC16** (pseudoenantiomer of **PTC14**, prepared from cinchonidine, see Supporting Information; 99% substrate conversion, 76% yield, 13:87 dr, entry 18, Table 1).

The superiority of catalysts **PTC8**, **PTC9**, **PTC15**, and **PTC16** (Table 1, entries 8, 9, and 15–18), all of which include an electron-withdrawing group on their benzyloxy residue, as opposed to relatively electron rich catalysts carrying a benzyloxy substituent (e.g., **PTC4**, entry 4, Table 1), is in line with Maruoka's inspirational work.²³ This trend is further corroborated with the observed superiority of catalysts **PTC39**, **PTC40**, and **PTC41** (all of which contain fluorine atoms on their benzyloxy residue, see Supporting Information) over **PTC38**, whose benzyloxy moiety includes an electron-rich residue (i.e., Me; see Supporting Information).

Striving for higher asymmetric induction and efficiency and beyond catalyst and alkylating agent absolute configuration optimization, we then investigated the effect of reaction conditions and catalyst loading on the alkylation of anthrone **7** with TBS-protected alkylating agent (*R*)-**8** and catalyst **PTC15**. Table 2 summarizes the results of this study that involved changes in the aqueous base, organic solvent, temperature, reaction time, and catalyst loading. Initial experiments (entries 1–6, Table 2) led to the identification of 40% aqueous Cs₂CO₃ and CH₂Cl₂ as the optimal base and solvent, respectively (entry 5, 0 °C, 10 mol % cat., 75% yield, 92:8 dr, Table 2). Changing the solvent from CH₂Cl₂ to (CH₂)₂Cl₂ increased the dr slightly (93:7, entry 7, Table 2), while decreasing the temperature steadily

from 0 to $-30\text{ }^{\circ}\text{C}$ led to further improvements in the dr with proportional increases in reaction time as expected (93:7; 94:6; 95:5; entries 12–14, respectively, Table 2). Stepwise decrease of catalyst loading from 10 to 0.1 mol % resulted in a slight increase of efficiency, albeit at the expense of reaction time (95:5–96:4 dr, entries 14–16, Table 2). The lower yield (due to decreased rate and conversion) reflected in entry 16 (Table 2, 15% yield) with 0.1 mol % catalyst loading provided an unacceptable limit, thereby leading us to adopt the 0.5 mol % catalyst loading as the most practical with regard to reaction rate, yield, and diastereoselectivity (72% yield, 95:5 dr, 40% aqueous Cs_2CO_3 , $(\text{CH}_2)_2\text{Cl}_2$, $-30\text{ }^{\circ}\text{C}$, 180 h, entry 17, Table 2).

Inspired by the effect of the chirality of the alkylating agent on the diastereoselectivity of the anthrone alkylation reaction as described above (Table 1), we set out to investigate a series of allylic bromides (**R**)-**8** varying in size of silyl protecting groups. For this investigation, we adopted catalyst **PTC15** and the conditions of entry 18 rather than those of entry 17 (Table 2) due to the shorter reaction time (for convenience). As shown in Table 3, the results of this study indicated a correlation between the bulkiness of the silyl protecting group and asymmetric induction. Thus, the most effective groups inducing the highest diastereoselectivities were those leading to products **6d** [tris(trimethylsilyl)silyl: 95:5 dr, 55% yield], **6b** (hexyldimethylsilyl: 95:5 dr, 74% yield), and **6** (*tert*-butyldimethylsilyl: 94:6 dr, 72% yield). Because of the lower yield of the reaction with tris(trimethylsilyl)silyl-protected allylic bromide (**R**)-**8d**, alkylating agents (**R**)-**8b** (hexyldimethylsilyl), and (**R**)-**8** (*tert*-butyldimethylsilyl) were chosen as the most attractive for further optimization.

The absolute configuration of substituted anthrone **6a** (mp $165\text{--}166\text{ }^{\circ}\text{C}$) obtained from the diastereoselective alkylation of anthrone **5**, allylic bromide (**R**)-**8a**, and **PTC15** as described in Table 3 was determined by X-ray crystallographic analysis (ORTEP, Figure 3, and CIF in the Supporting Information).²⁰ Indeed, the crystallization of **6a** that allowed its absolute configuration assignment at this point was a fortunate event, since all other products in Table 3 were foams in nature.

Finally, we explored the C1 and C5 substituent effects on the diastereoselectivity of the anthrone alkylation using hexyldimethylsilyl-protected bromide (**R**)-**8b**, anthrones **7**, **7i–7p**, and **PTC15** under the optimized conditions as shown in Table 4. These studies revealed that substituents at the C1 position of the anthrone substrates smaller than OBn (i.e., **6b**, 95:5 dr) resulted in decreased diastereoselectivities (i.e., **6i**: 90:10 dr; **6j**: 93:7 dr), while larger substituents at this position led to increased diastereoselectivities (e.g., **6k**: 92:8 dr; **6l**: 98:2 dr). The significant increase in diastereoselectivity for product **6l** carrying the *p*-trifluoromethyl benzyloxy group was notable, and a benzyloxy group at C5 (i.e., **6m**) instead of methoxy increased the diastereoselectivity to 99:1 dr led to even more impressive improvements. Thus, the highest diastereoselectivities were obtained for the combinations of anthrone substrates (**7n**, **7o**, and **7p**) and alkylating agent (**R**)-**8b**, which led to highly enantioenriched products **6n** (>99:1 dr), **6o** (99:1 dr), and **6p** (>99:1 dr) as shown in Table 4.

2.2. Enantioselective Total Synthesis and Absolute Configuration of (–)-Viridicatumtoxin B

Having developed an efficient and highly enantioselective synthesis of 10-substituted anthrones, we were in a position to undertake the total synthesis of enantiopure viridicatumtoxin B in an attempt to determine its absolute configuration. Given that the literature reports on the structures of viridicatumtoxin A (**2**, Figure 1; absolute configuration confirmed by X-ray crystallographic analysis)⁵ and spirohexaline³ (**3**, reported structure shown in Figure 1) suggested opposite absolute configurations for these two siblings, we were ambivalent as to which absolute configuration of viridicatumtoxin B to target first. Since our asymmetric synthesis of anthrones revealed a higher diastereoselectivity for **PTC15** (leading to the corresponding C10-substituted anthrones, see Table 1) than that for **PTC16** (leading to the antipodal enantiomer), we decided to employ the former as a means to reach one of the enantiomers of viridicatumtoxin B (**1**).

To this end, we adopted substrate anthrone **7**, alkylating agent allylic bromide (**R**)-**8**, and catalyst **PTC15** in our attempt to construct the first chiral intermediate (**6S,17R**)-**6** and convert it stereospecifically to the pending intermediate, spirocyclic (**6S,15R**)-**4**, enroute to viridicatumtoxin B (Scheme 1). It was with considerable trepidation that we pondered the latter possibility, given the sensitivity of the substrate and the conditions involved in this spirocyclization. As shown in Scheme 1, the reaction of anthrone **7** (3.01 g, 8.00 mmol) with allylic bromide (**R**)-**8** (3.06 g, 8.80 mmol) under the influence of **PTC15** (0.5 mol %) was carried out on gram scale, delivering the expected substituted anthrone (**6S,17R**)-**6** in 72% yield and 95:5 dr. The latter was subjected to optimized Lewis acid mediated spirocyclization conditions (BF₃·Et₂O, 5 mol %) to afford spirocyclic (**6S,15R**)-**4** in 74% yield and, much to our delight, with no loss of enantiopurity (95:5 er, see details in Supporting Information). Recrystallization of (**6S,15R**)-**4** from hexanes/CH₂Cl₂ (50:1) led to further enantioenrichment of this intermediate (>99:1 er). Failing attempts to prepare a crystalline, heavy-atom-containing derivative of (**6S,15R**)-**4** for absolute configuration determination purposes (including the newly formed spirocenter), we subjected the latter first to the action of diacetoxyiodo-benzene (PIDA) and then to camphorsulfonic acid (CSA) in MeOH/CH₂Cl₂, conditions that led to *p*-quinomethide (–)-**9** (via the corresponding dimethoxyketal) in 81% overall yield. Treatment of (–)-**9** with *p*-bromobenzoyl chloride under basic conditions furnished crystalline derivative (–)-**11** (mp 220–221 °C), whose single crystal X-ray crystallographic analysis (ORTEP, Scheme 1, and CIF in the Supporting Information)²¹ revealed that indeed the single stereocenter (C15, viridicatumtoxin numbering) within intermediate (–)-**9** (to be converted to viridicatumtoxin B) was of the shown chirality. Chiral HPLC analysis confirmed its homogeneity as a single enantiomer (see details in Supporting Information). This absolute configuration corresponds to that suggested for spirohexaline (**3**),³ rather than that determined for viridicatumtoxin A (**2**).⁵

The faithful transfer of absolute configuration from C6 (viridicatumtoxin numbering) in intermediate (**6S,17R**)-**6** to C15 in (**6S,15R**)-**4** is the consequence of the carbonium-mediated spirocyclization that requires attack of the C7 position on the aromatic ring onto C15 carbonium ion from the “top” side of a sterically controlled transition state (**A**: preferred; **B**: sterically congested), in which the *gem*-dimethyl groups play a non-negotiable steric control (see Figure 4).

Our intention to obtain both enantiomeric forms of viridicatumtoxin B prompted us to push on with this enantiomer of key building block (–)-**9**, whose absolute configuration we just determined and whose single stereocenter (**15R**) was destined to control the stereochemistry of all others en route to the targeted molecule. We also took the opportunity along the way to optimize the process from the original one that delivered racemic viridicatumtoxin B (**1**).⁴ Scheme 2 summarizes the optimized synthesis of what turned out to be (–)-viridicatumtoxin B [(–)-**1**] starting with enantiopure precursor (–)-**9**. Thus, dearomatization of (–)-**9** with PIDA in MeOH/CH₂Cl₂ furnished, in 90% yield, dimethoxy semiquinone (–)-**12**. In an effort to improve the previously low diastereoselectivity (ca. 2:1 dr)⁴ of the coupling of racemic **12** with oxazoline **5**, we performed the reaction (*t*-BuOK, –50 °C, 48 h) in the presence of chiral catalyst **PTC14** in the hope that the latter would exert a degree of stereocontrol. It was indeed with pleasure that we observed the formation of the expected heptacycle product (+)-**13**, in 88% yield and ca. 4:1 dr, as opposed to 91% yield and ca. 2:1 dr in the original procedure, a welcome improvement since the major diastereoisomer was the desired one shown in Scheme 2. Complexation of ligand **PTC14** with the initially formed anion of oxazoline **5** followed by preferred attack on substrate (–)-**12** from the “bottom” side may explain the observed diastereoselectivity. For clarity, we note that the diastereoselectivity in this reaction refers to the C15 and C4/C4a stereocenters with the latter being of the *syn* configuration with respect to the H-residue on C4a. The 4:1 mixture of Teoc derivative (+)-**13** was transformed to decarboxylated ketoenol (–)-**14** as previously described.⁴ The hydroxylation of (–)-**14** was improved in terms of yield and diastereoselectivity from the original (36%, 2:1 dr, 60% based on recovered starting material) through optimized conditions [THF, 0.2 equiv of Ni(acac)₂, 3.0 equiv of DMDO, THF, –78 °C, 3 h, 52%, 4:1 dr, 72% based on recovered starting material]. This improvement may be attributed to increased reactivity of Ni(acac)₂ in THF as solvent (as opposed to the originally used CH₂Cl₂), an effect that resulted in a cleaner and faster reaction. The reduction of (–)-**15** (4:1 diastereomeric mixture) with NaCNBH₃ allowed convenient chromatographic separation of resulting isomeric products (+)-**16** and (–)-**17**, with the latter (and desired) now obtained from (–)-**13** with improved overall diastereoselectivity (ca. 4:1) as opposed to ca. 2:1 in the original route.⁴ The ketal hydrolysis of major isomer (–)-**17** with aqueous HCl proceeded well to afford hydroxy triketone (–)-**18**, whose regioselective reduction with NaBH(OAc)₃ furnished dihydroxy diketone (–)-**19** (46% yield). Optimization of conditions of the ensuing silylation of the latter with TBSOTf and 2,6-lutidine led to an improved yield of TBS-ether (+)-**20** (76% vs 61%).⁴ The crucial hydroxylation of (+)-**20** was also improved over that of the original procedure⁴ (32% yield, 55% based on 42% recovered starting material) by optimization of conditions that included freshly prepared Davis oxaziridine reagent. The recruiting steps proceeded as previously reported for the racemic series⁴ to provide enantiopure (–)-viridicatumtoxin B [(–)-**1**] through intermediates (–)-**22** (HF·py, 72% yield; existing as an equilibrium mixture with its 1,5-lactol isomeric form (–)-**22'**) and (–)-**23**. The latter intermediate was obtained in 82% yield (as compared to 66% for the previous procedure)⁴ by adding the DMP as a solution in CH₂Cl₂ slowly and in portions, thereby resulting in further improvement in the process. Finally, exposure of precursor (–)-**23** to hydrogenolysis conditions (H₂, Pd black) furnished the coveted viridicatumtoxin B, whose levorotatory nature ($[\alpha]_D^{22} = -116, c=0.1, \text{EtOH}$) led

to its absolute configuration assignment as enantiomer [(-)-**1**] of the natural product. Besides pointing to the absolute configuration of natural viridicatumtoxin B, this observation cast doubts over the depicted absolute configuration of spirohexaline in the isolation paper.³

2.3. Enantioselective Total Synthesis and Absolute Configuration of (+)-Viridicatumtoxin B

With an enantioselective and improved synthetic route at hand, the road to what was sure to be the correct enantiomer of viridicatumtoxin B was now open. For optimum results we chose to use, in addition to anthrone **7**, the (*S*)-enantiomer of allylic bromide **8** [(*S*)-**8**], and the new catalyst **PTC17** (derived from quinine), the latter being the pseudoenantiomer of **PTC15** (derived from quinidine) rather than **PTC16** that was used in the methodology development study described above (see Table 1). Equipped with the phenolic moiety on its quinoline domain, **PTC15** proved its superiority over **PTC16**, which lacks this phenolic group, as seen in Table 1 (entries 17 and 18). This crucial observation prompted us to synthesize **PTC17** (Scheme 3; for details of the synthesis, see Supporting Information), as we expected it to perform better than **PTC16** in the anthrone alkylation step.

Indeed, as shown in Scheme 3, catalyst **PTC17** performed well in ensuring high diastereoselectivity in the alkylation of anthrone **7** (6.02 g scale, 16.0 mmol) with allylic bromide (*S*)-**8**, affording alkylated anthrone (**6R,17S**)-**6** in 72% yield and 95:5 dr (as opposed to 87:13 dr obtained with **PTC16**, see Table 1, entry 18). The obtained product was purified by recrystallization from hexanes, the racemate crystallizing out of the solution and the enriched material [i.e., (**6R,17S**)-**6**] being recovered from the mother liquor. The latter was then subjected to the developed spirocyclization reaction conditions [BF₃·Et₂O (cat.)] furnishing pentacycle (**6R,15S**)-**4** as expected. The absolute configuration of this intermediate was determined by conversion to its *p*-bromobenzoate derivative (+)-**11**, obtained via intermediate (+)-**9**, as summarized in Scheme 3. The X-ray crystallographic analysis (ORTEP representation, Scheme 3, and CIF in the Supporting Information)²² of (+)-**11** (mp 220–221 °C) confirmed its (*S*) absolute configuration as expected from the results shown in Scheme 3 for its enantiomer.

The total synthesis of (+)-viridicatumtoxin B [(+)-**1**] from key building block spiropentacycle (+)-**9** was successfully carried out through the same route and conditions (Figure 5), and in similar yields, as those employed for its enantiomeric form [(-)-**1**] (see Scheme 3 and the Supporting Information for more details). Synthetic viridicatumtoxin B exhibited the same sign of optical rotation as the one reported in the literature for the natural substrate { [α]_D²² = +118, *c* = 0.1, EtOH for synthetic (+)-**1**; [α]_D²² = +18.3, *c* = 0.2, EtOH for natural (+)-**1**}.¹ The higher value for the synthetic material may reflect its higher purity, while the lower value reported for the natural substance may be due to purification and measurement difficulties due to its low natural abundance.¹ However, the possibility of the latter occurring in nature in its scalemic form cannot be excluded at this time.

2.4. Enantioselective Synthesis of Viridicatumtoxin B Analogues

With a practical and enantioselective route to viridicatumtoxin B [(+)-**1**] and its antipode [(-)-**1**] and their precursors available to us, we decided to apply it to the construction of a number of their enantiopure analogues (see Figure 6).

We were particularly interested in comparing the antibacterial properties of the antipodal simpler viridicatumtoxin analogues shown in Figure 6 [(+)-**VA1**, (-)-**VA2**, (+)-**VA3**, (-)-**VA4**, (-)-**VA5**, (+)-**VA6**, (-)-**VA7**, (+)-**VA8**, (+)-**VA9**, (-)-**VA10**, (-)-**VA11**, and (+)-**VA12**]. Their synthesis proceeded smoothly from their required precursors, all of which were encountered in our synthetic studies toward (+)- and (-)-viridicatumtoxin B as described above.

Scheme 4 summarizes the synthesis of (+)-**VA1** and (+)-**VA3** from precursor (-)-**17**. Thus, reduction of precursor (-)-**17** with NaCNBH₃ in AcOH at ambient temperature resulted in the formation of a mixture of 5 β -methyl ether (+)-**24** (48% yield) and its epimer 5 α -methyl ether (-)-**5-epi-24** (32% yield), which were chromatographically separated. Hydrogenolysis of (+)-**24** with Pd black as a catalyst then furnished viridicatumtoxin B analogue (+)-**VA1** in 95% yield. Similar treatment of (-)-**5-epi-24** led to analogue (+)-**VA3** in comparable yield as for (+)-**VA1** (see Scheme 4). Analogues (-)-**VA5** and (-)-**VA7** were prepared from precursor (+)-**16** in two steps, while the NaCNBH₃ reduction gave (-)-**4a,12a-epi-24** in 17% yield and (+)-**5,4a,12a-epi-24** in 51% yield, and the following hydrogenolysis of each produced analogues (-)-**VA5** and (-)-**VA7** in similar yields (see Scheme 5). Analogues (-)-**VA2** and (-)-**VA4** were similarly prepared from their precursor (+)-**17** in yields comparable to those for (+)-**VA1** and (+)-**VA3** as summarized in Scheme 6. Analogues (+)-**VA6** and (+)-**VA8** were similarly prepared from their precursor (-)-**16** in yields comparable to those for (-)-**VA5** and (-)-**VA7** as summarized in Scheme 7. Analogue (+)-**VA9** was obtained by hydrogenolysis of triketone (-)-**18** in 95% yield (Scheme 8, A). Analogue (-)-**VA11** was synthesized from hydrolysis of precursor (+)-**16** (quant. yield), followed by hydrogenolysis with Pd black (Scheme 8, B). Analogues (-)-**VA10** and (+)-**VA12** were similarly prepared from their respective precursors as summarized in Scheme 8 C,D.

2.5. Biological Evaluation of Synthetic (+)- and (-)-Viridicatumtoxin B and Analogues

The synthesized simpler enantiopure analogues (+)-**VA1**, (-)-**VA2**, (+)-**VA3**, (-)-**VA4**, (-)-**VA5**, (+)-**VA6**, (-)-**VA7**, (+)-**VA8**, (+)-**VA9**, (-)-**VA10**, (-)-**VA11**, and (+)-**VA12** (see Figure 6 for structures), all lacking the C4 α -hydroxyl group so cumbersome to install, together with (+)- and (-)-viridicatumtoxin B [(+)-**1** and (-)-**1**] were tested against a number of bacterial strains and compared to natural viridicatumtoxin B [(+)-**1**, taking reported values from ref¹ for *Enterococcus faecalis* KCTC5191, *Enterococcus faecium* KCTC3122, methicillin-resistant *Staphylococcus aureus* CCARM3167 (MRSA CCARM3167), *Acinetobacter calcoaceticus* KCTC2357, and *Escherichia coli* CCARM1356], minocycline (Minocin, **CK1**), and tigecycline (Tygacil, **CK2**) (see Figure 7 for structures).

As shown in Table 5, most of the viridicatumtoxins and analogues tested exhibited antibacterial efficacy against Gram-positive bacteria [(*E. faecalis* S613, *E. faecium* 105, and methicillin-resistant *S. aureus* 371 (MRSA 371)] but were less active against Gram-negative bacteria (i.e., *Acinetobacter baumannii* AB210). Thus, synthetic viridicatumtoxins B [(+)-**1** and (-)-**1**] exhibited comparable antibacterial properties against these strains [*E. faecalis* S613, *E. faecium* 105, and MRSA 371: MIC = 2, 2, and 4 μ g/mL, respectively, for (+)-**1**; MIC = 4, 4, and 8 μ g/mL, respectively, for (-)-**1**] to those reported¹ for natural viridicatumtoxin B [(+)-**1**] against similar strains (*E. faecalis* KCTC5191, *E. faecium*

KCTC3122, MRSA CCARM3167: MIC = 2, 0.5, and 0.5 $\mu\text{g}/\text{mL}$, respectively). Based on these data, it seems that synthetic (+)-viridicatumtoxin B [(+)-**1**] is twice as potent as its antipode (-)-viridicatumtoxin B [(-)-**1**]. The Clinical and Laboratory Standards Institute (CLSI) states that MIC testing has a 2-fold error, which makes the values for (+)-viridicatumtoxin B and (-)-viridicatumtoxin B within the error range for their MIC values. Nonetheless, (+)-viridicatumtoxin B displayed high activity against the Gram-positive strains across the three independent replicates.

For the 5-methoxy analogues (+)-**VA1**, (-)-**VA2**, (+)-**VA3**, (-)-**VA4**, (-)-**VA5**, (+)-**VA6**, (-)-**VA7**, and (+)-**VA8**, potencies against the tested strains were generally lower than those of synthetic viridicatumtoxin B [(+)-**1**], except for analogue (+)-**VA6**, which exhibited comparable potencies against *E. faecalis* S613 (MIC = 1 $\mu\text{g}/\text{mL}$) and *E. faecium* 105 (MIC = 2 $\mu\text{g}/\text{mL}$). However, all four 5,12-diketo analogues [(+)-**VA9**, (-)-**VA10**, (-)-**VA11**, and (+)-**VA12**] demonstrated antibacterial properties stronger than those of synthetic viridicatumtoxin B [(+)-**1**] against *E. faecalis* S613 [(+)-**VA9**: MIC = 0.5 $\mu\text{g}/\text{mL}$; (-)-**VA10**: MIC = 1 $\mu\text{g}/\text{mL}$; (-)-**VA11**: MIC = 1 $\mu\text{g}/\text{mL}$; (+)-**VA12**: MIC = 1 $\mu\text{g}/\text{mL}$], *E. faecium* 105 [(+)-**VA9**: MIC = 2 $\mu\text{g}/\text{mL}$; (-)-**VA10**: MIC = 1 $\mu\text{g}/\text{mL}$; (-)-**VA11**: MIC = 0.5 $\mu\text{g}/\text{mL}$; (+)-**VA12**: MIC = 1 $\mu\text{g}/\text{mL}$], and MRSA 371 [(+)-**VA9**: MIC = 2 $\mu\text{g}/\text{mL}$; (-)-**VA10**: MIC = 2 $\mu\text{g}/\text{mL}$; (-)-**VA11**: MIC = 2 $\mu\text{g}/\text{mL}$; (+)-**VA12**: MIC = 2 $\mu\text{g}/\text{mL}$] (see Table 4). These results are significant in that they show that (a) the C-4a hydroxyl group of the viridicatumtoxin B molecule is not necessary for antibacterial activity and (b) the chirality of the molecule is not important for the tested bioactivity.

The modified synthetic route delivers enantiopure viridicatumtoxin B in 0.985% overall yield from key building block **7** as compared to 0.267% yield for the original route to racemic viridicatumtoxin B from the same prochiral intermediate (**7**), thus resulting in a 3.7-fold improved efficiency. Furthermore, these studies revealed a potential drug candidate [i.e., (-)-**VA10**] that is biologically superior and molecularly simpler than viridicatumtoxin B. This analogue can be derived from precursor **32** in one step and 95% yield as opposed to the natural product that requires six steps for its generation from the same intermediate in only 11% overall yield. These improvements bode well for compound (-)-**VA10** and its siblings [such as (+)-**VA9**, (-)-**VA11**, and (+)-**VA12**] as potential drug candidates for further development. Despite the previously reported activity of viridicatumtoxin B against several Gram-negative bacterial strains,¹ our tested compounds proved inactive against *A. baumannii* AB210. Further improvements of the antibacterial and pharmacological profiles of these compounds may be achieved by incorporating beneficial structural motifs such as the C4-dimethylamino group, which proved important for imparting the broad-spectrum activity observed for both minocycline (**CK1**) and tigecycline (**CK2**).²³

3. CONCLUSION

An efficient and practical catalytic asymmetric alkylation of anthrones with cyclic allylic bromides and new phase transfer catalysts derived from quinidine and quinine has been developed. Achieving up to 99.6:0.4 selectivities and employing as low as 0.5 mol % catalyst, this method was applied to the total synthesis of both enantiomeric forms of viridicatumtoxin B. Guided by X-ray crystallographic analysis of precursor intermediates

that revealed their absolute configurations and the signs of optical rotations of synthetic and natural viridicatumtoxin B (**1**),¹ the absolute configuration of this antibiotic was deduced. This configuration is in agreement with that of viridicatumtoxin A (**2**) determined by X-ray crystallographic analysis and reported in 1982.²⁰ However, it differs from that depicted for spirohexaline (**3**),^{3,23} a closely related member of the viridicatumtoxin family of natural products. Since no experimental data were reported for the given structure to spirohexaline (**3**),³ we suggest that its absolute configuration is most likely the same as those of viridicatumtoxins B (**1**) and A (**2**). The developed catalytic asymmetric alkylation of anthrones may find applications in organic synthesis in general, while its application to the synthesis of enantiopure natural or designed members of the viridicatumtoxin class and related compounds may lead to attractive and urgently needed drug candidates to be developed as new antibacterial agents to combat menacing infections by drug-resistant bacteria. Simpler viridicatumtoxin B analogues (+)-**VA9**, (-)-**VA10**, (-)-**VA11**, and (+)-**VA12** are attractive candidates for further investigation along these lines.

Supplementary Material

Refer to Web version on PubMed Central for supplementary material.

Acknowledgments

Financial support for this work was provided by the National Institutes of Health (USA) (grant AI055475), the Cancer Prevention & Research Institute of Texas (CPRIT), and The Welch Foundation (grant C1819). A fellowship from the Postdoctoral International Exchange Program of China Postdoctoral Science Foundation (CPSF) to G.L. is gratefully acknowledged. We thank Prof. W. G. Kim for graciously providing us with copies of ¹H and ¹³C NMR spectra of natural viridicatumtoxin B. We also thank Dr. L. B. Alemany and Dr. Q. Kleerekoper from Rice University and Mrs. Tamara Meinel, and Dr. Lothar Hennig from Leipzig University for NMR spectroscopic assistance, Dr. J. D. Korp (University of Houston) for X-ray crystallographic analysis assistance, and Dr. I. Riddington (University of Texas at Austin) and Dr. C. Pennington (Rice University) for mass spectrometric assistance.

References

1. Zheng CJ, Yu HE, Kim EH, Kim WG. *J Antibiot.* 2008; 61:633–637. [PubMed: 19168978]
2. Hutchison RD, Steyn PS, van Rensburg SJ. *Toxicol Appl Pharmacol.* 1973; 24:507–509. [PubMed: 4122267]
3. Inokoshi J, Nakamura Y, Hongbin Z, Uchida R, Nonaka K, Masuma R, Tomoda H. *J Antibiot.* 2013; 66:37–41. [PubMed: 23168407]
4. (a) Nicolaou KC, Nilewski C, Hale CRH, Ioannidou HA, ElMarrouni A, Koch LG. *Angew Chem, Int Ed.* 2013; 52:8736–8741. (b) Nicolaou KC, Hale CRH, Nilewski C, Ioannidou HA, ElMarrouni A, Nilewski LG, Beabout K, Wang TT, Shamoo Y. *J Am Chem Soc.* 2014; 136:12137–12160. [PubMed: 25317739]
5. Silverton JV, Kabuto C, Akiyama T. *Acta Crystallogr, Sect B: Struct Crystallogr Cryst Chem.* 1982; 38:3032–3037.
6. For reviews on Pd-catalyzed asymmetric alkylations, see (a) Trost BM, Machacek MR, Aponick A. *Acc Chem Res.* 2006; 39:747–760. [PubMed: 17042475] (b) Trost BM. *J Org Chem.* 2004; 69:5813–5837. [PubMed: 15373468] (c) Trost BM, Crawley ML. *Chem Rev.* 2003; 103:2921–2944. [PubMed: 12914486] (d) Trost BM, Van Vranken DL. *Chem Rev.* 1996; 96:395–422. [PubMed: 11848758] (e) Trost BM. *Acc Chem Res.* 1996; 29:355–364.
7. For selected reviews on asymmetric phase-transfer catalysis, see (a) Maruoka K, Ooi T. *Chem Rev.* 2003; 103:3013–3028. [PubMed: 12914490] (b) Ooi T, Maruoka K. *Angew Chem, Int Ed.* 2007; 46:4222–4266.

8. Trost BM, Bunt RC. *J Am Chem Soc.* 1994; 116:4089–4090.
9. Shih HW, Vander Wal MN, Grange RL, MacMillan DWC. *J Am Chem Soc.* 2010; 132:13600–13603. [PubMed: 20831195]
10. (a) Liu Y, Provencher BA, Bartelson KJ, Deng L. *Chem Sci.* 2011; 2:1301–1304. [PubMed: 22174974] (b) Provencher BA, Bartelson KJ, Liu Y, Foxman BM, Deng L. *Angew Chem, Int Ed.* 2011; 50:10565–10569.
11. Ceban V, Tauchman J, Meazza M, Gallagher G, Light ME, Gergelitsová I, Veselý J, Rios R. *Sci Rep.* 2015; 5:16886. [PubMed: 26592555]
12. (a) Corey EJ, Xu F, Noe MC. *J Am Chem Soc.* 1997; 119:12414–12415. (b) Corey EJ, Bo Y, Busch-Petersen J. *J Am Chem Soc.* 1998; 120:13000–13001.
13. Kitamura M, Shirakawa S, Maruoka K. *Angew Chem, Int Ed.* 2005; 44:1549–1551.
14. Iwabuchi Y, Nakatani M, Yokoyama N, Hatakeyama S. *J Am Chem Soc.* 1999; 121:10219–10220.
15. (a) Lee TBK, Wong GSK. *J Org Chem.* 1991; 56:872–875. (b) Lian M, Li Z, Du J, Meng Q, Gao Z. *Eur J Org Chem.* 2010; 34:6525–6530.
16. (a) Kobbelgaard S, Bella M, Jørgensen KA. *J Org Chem.* 2006; 71:4980–4987. [PubMed: 16776530] (b) Liang J, Pan J, Xu D, Xie J. *Tetrahedron Lett.* 2014; 55:6335–6338.
17. (a) Zeng X, Miao C, Wang S, Xia C, Sun W. *Chem Commun.* 2013; 49:2418–2420. (b) Adam W, Rao PB, Degen HG, Levai A, Patonay T, Saha-Möller CR. *J Org Chem.* 2002; 67:259–264. [PubMed: 11777469] (c) Xie JW, Xu ML, Zhang RZ, Pan JY, Zhu WD. *Adv Synth Catal.* 2014; 356:395–400.
18. (a) Johnston CP, Kothari A, Sergeieva T, Okovytyy SI, Jackson KE, Paton RS, Smith MD. *Nat Chem.* 2015; 7:171–177. (b) Li M, Woods PA, Smith MD. *Chem Sci.* 2013; 4:2907–2911.
19. Corey EJ, Bakshi RK, Shibata S. *J Am Chem Soc.* 1987; 109:5551–5553.
20. CCDC 1447911 contains the supplementary crystallographic data of **6a** for this paper. These data can be obtained free of charge from The Cambridge Crystallographic Data Centre.
21. CCDC 1503479 contains the supplementary crystallographic data of (–)-**11** for this paper. These data can be obtained free of charge from The Cambridge Crystallographic Data Centre.
22. CCDC 1503480 contains the supplementary crystallographic data of (+)-**11** for this paper. These data can be obtained free of charge from The Cambridge Crystallographic Data Centre.
23. Nelson, M. Hillen, W., Greenwald, RA., editors. *Tetracyclines in Biology, Chemistry, and Medicine.* Birkhauser Verlag; Basel: 2001. p. 26

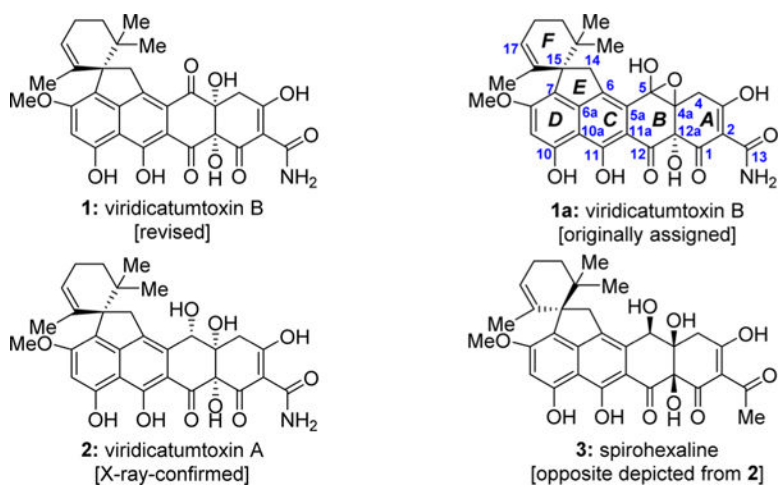


Figure 1.
Molecular structures of viridicatumtoxins (**1** and **2**) and spirohexaline (**3**).

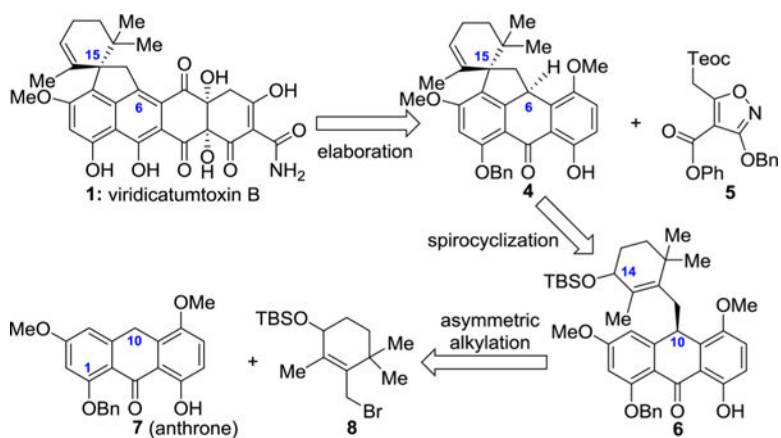


Figure 2. Proposed asymmetric total synthesis of viridicatumtoxin B through asymmetric alkylation of anthrone **7** with allylic bromide **8** in retrosynthetic format (labeling of **1** based on viridicatumtoxin B numbering; labeling of **6** and **7** based on anthrone numbering).

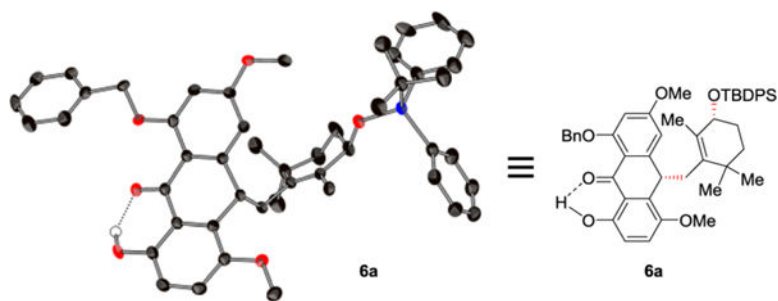


Figure 3.
X-ray derived ORTEP representation of **6a**.

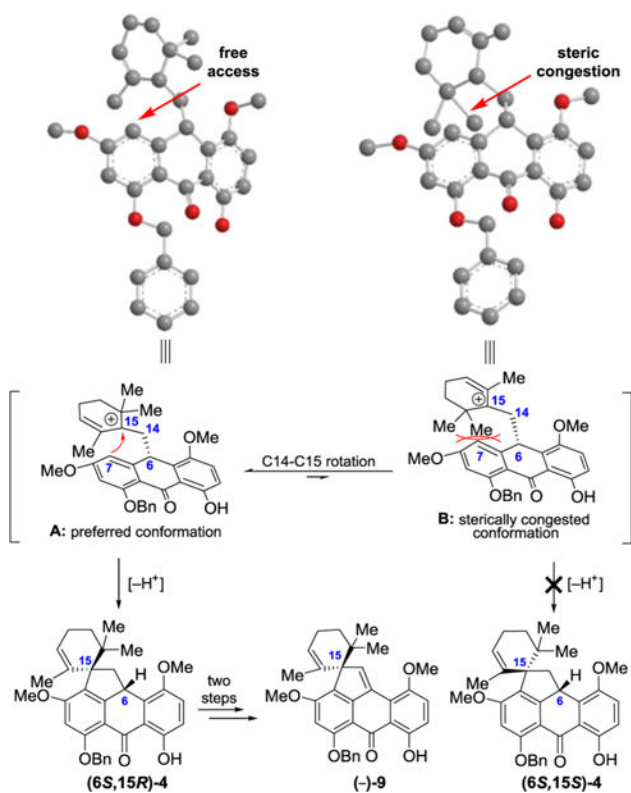


Figure 4. Proposed mechanism of stereoselective spirocyclization of substituted anthrone **(6S,17R)-6** to pentacycle **(6S,15R)-4** through carbonium species **A** (viridicatumtoxin numbering for all intermediates and compounds).

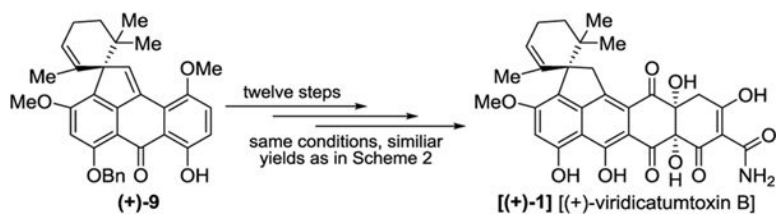


Figure 5.
Total synthesis of enantiopure (+)-viridicatumtoxin B [(+)-1].

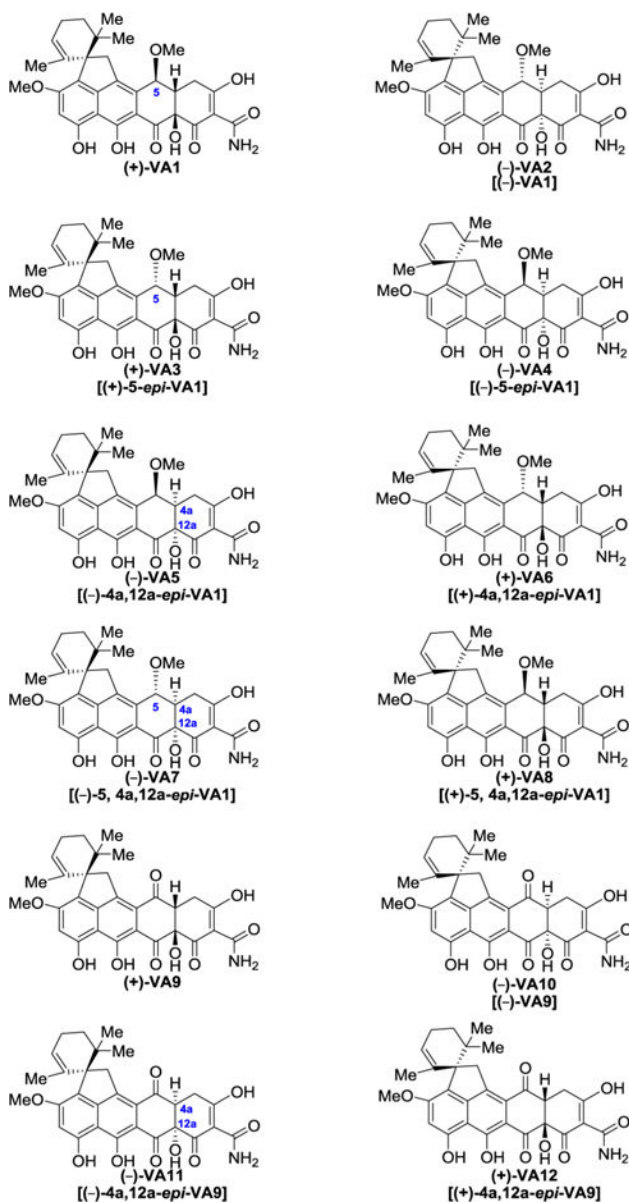


Figure 6. Synthesized viridicutumtoxin B analogues (+)-VA1, (-)-VA2, (+)-VA3, (-)-VA4, (-)-VA5, (+)-VA6, (-)-VA7, (+)-VA8, (+)-VA9, (-)-VA10, (-)-VA11, and (+)-VA12.

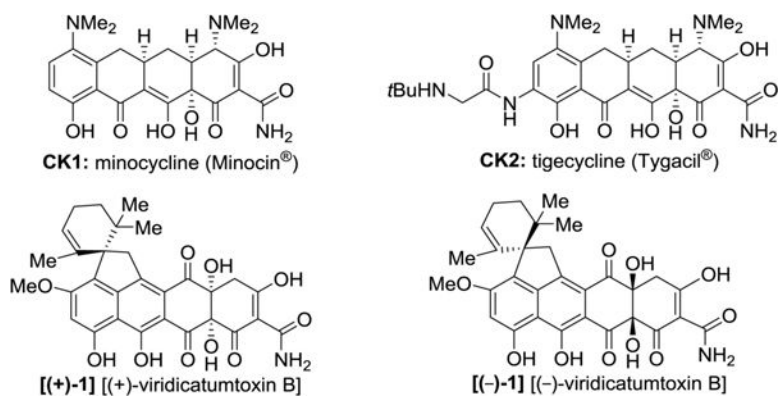
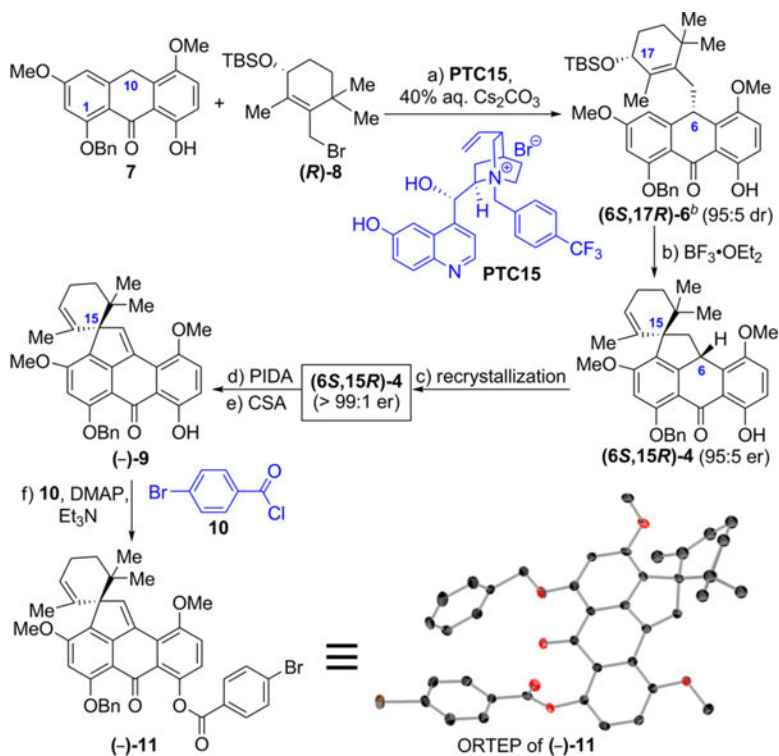
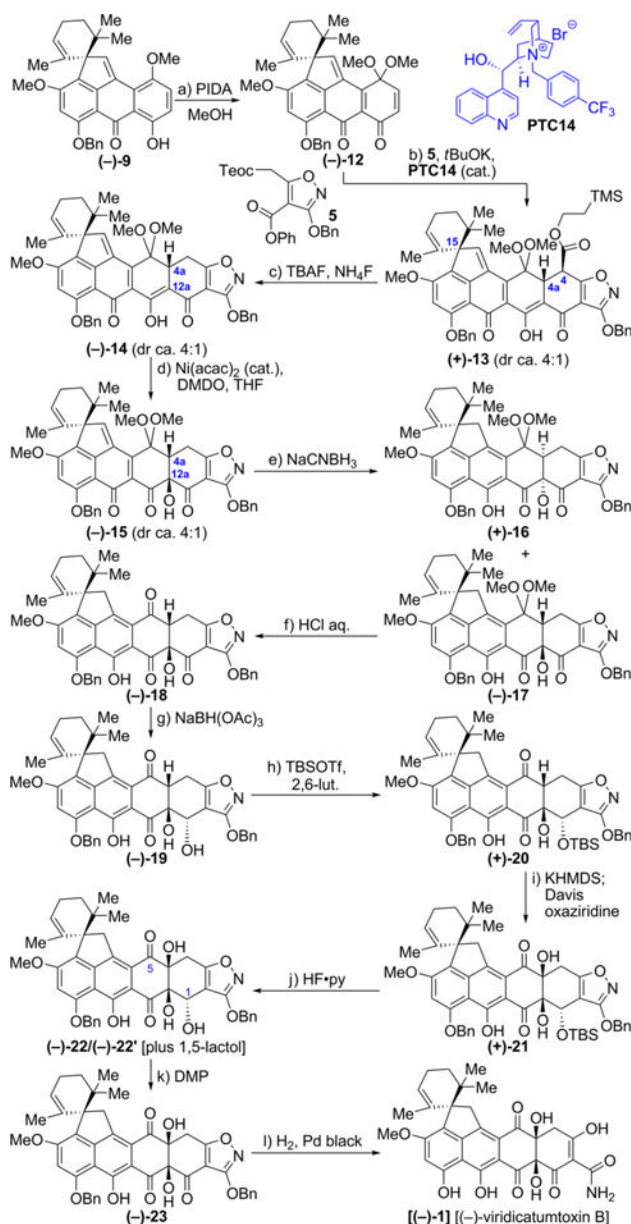


Figure 7. Molecular structure of tetracycline drugs minocycline (**CK1**), tigecycline (**CK2**), and (+)- and (-)-viridicatumtoxin B [(+)-**1** and (-)-**1**].



Scheme 1. Enantioselective Synthesis of the BCDEF Fragment (*6S,15R*)-4 of (-)-Viridicatumtoxin B [(-)-1] and Its Absolute Configuration^a

^aReagents and conditions: (a) **7** (3.01 g, 8.00 mmol scale), **PTC15** (0.5 mol %) 40% aqueous Cs_2CO_3 , $(\text{CH}_2)_2\text{Cl}_2$, -30°C , 10 days, 72%, 95:5 dr; (b) $\text{BF}_3 \cdot \text{Et}_2\text{O}$ (0.05 equiv), CH_2Cl_2 , -78 to 0°C , 30 min, 74%, 95:5 er; (c) hexanes/ CH_2Cl_2 (50:1), 91%, > 99:1 er; (d) PIDA (1.2 equiv), $\text{MeOH}/\text{CH}_2\text{Cl}_2$ (1:1), 0°C , 30 min, 25°C , 30 min; (e) CSA (0.07 equiv), CH_2Cl_2 , 0°C , 5 min, 81% for two steps; (f) **10** (5.0 equiv), DMAP (10 equiv), Et_3N (30 equiv), CH_2Cl_2 , 25°C , 6 h, 95%. ^bTo avoid confusion, the numbering on (*6S,17R*)-**6**, (*6S,15R*)-**4**, and (-)-**9** in this scheme and Figure 4 is based on the viridicatumtoxin numbering, as opposed to the carbon numbering of compound (*10S,14R*)-**6** (see Table 1), which is the same as (*6S,17R*)-**6**, the latter being designated using the anthrone numbering.



Scheme 2. Total Synthesis of Enantiopure (-)-Viridicatumtoxin B [(-)-1]^a

^aReagents and conditions: (a) PIDA (1.2 equiv), MeOH/CH₂Cl₂ (10:1), 25 °C, 1.5 h, 86%; (b) 5 (1.1 equiv), *t*-BuOK (1.2 equiv), **PTC14** (0.01 equiv), toluene, -50 °C, 48 h, 88%, 4:1 dr; (c) TBAF (10 equiv), NH₄F (20 equiv), degassed THF, 25 °C, 5 min, 87%, 4:1 dr; (d) [Ni(acac)₂] (0.2 equiv), DMDO (3.0 equiv), THF, -78 °C, 3 h, 52% (4:1 dr, 72% brsm), 28% recovered (-)-**14**; (e) NaCNBH₃ (4 equiv), THF, -78 °C, 1.5 h, 48% for (-)-**17**, 12% for (+)-**16**, chromatographically separated; (f) 2 N aqueous HCl, THF, 25 °C, 5 h, quant.; (g) NaBH(OAc)₃ (1.2 equiv), EtOAc/acetone (1:1), 40 °C, 2 h, 46%; (h) TBSOTf (4 × 10 equiv), 2,6-lutidine (4 × 15 equiv), CH₂Cl₂, 0 to 25 °C for four times, totaling 2 h, 76%; (i) KHMDS (3.4 equiv), THF, -78 °C, 1 h; then freshly prepared Davis oxaziridine (3.9 equiv), -78 °C, 2 h, 32% of (+)-**21** (55% brsm) + 42% recovered (+)-**20**; (j) HF-pyridine (excess, added at 0 °C in four portions), MeCN, 0 to 55 °C for four times, totaling 20 h, 72%

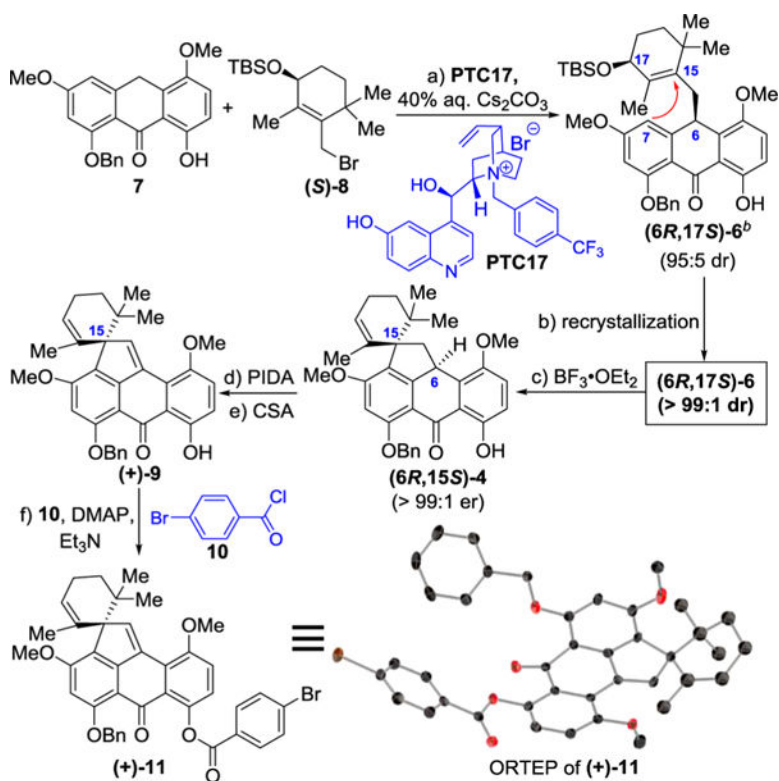
(product **22** exists in equilibrium with its 1,5-lactol isomeric form); (k) DMP solution in CH_2Cl_2 (0.3 M, 1.8 equiv, added in two portions at 0 °C), $(\text{CH}_2)_2\text{Cl}_2$, 0 to 50 °C two times, totaling 2 h, 82%; (l) H_2 , Pd black (4.9 equiv), 1,4-dioxane/MeOH (1:1), 25 °C, 10 min, 96%.

Author Manuscript

Author Manuscript

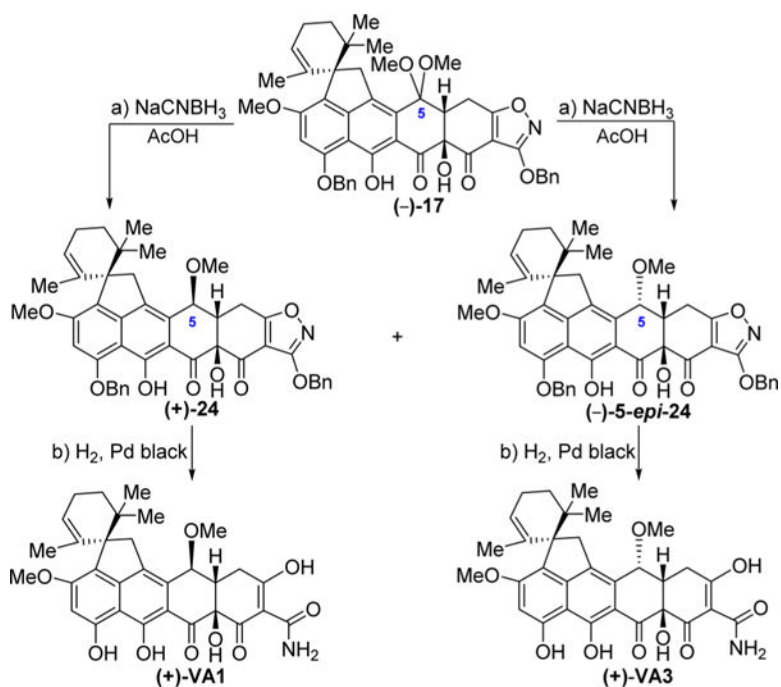
Author Manuscript

Author Manuscript



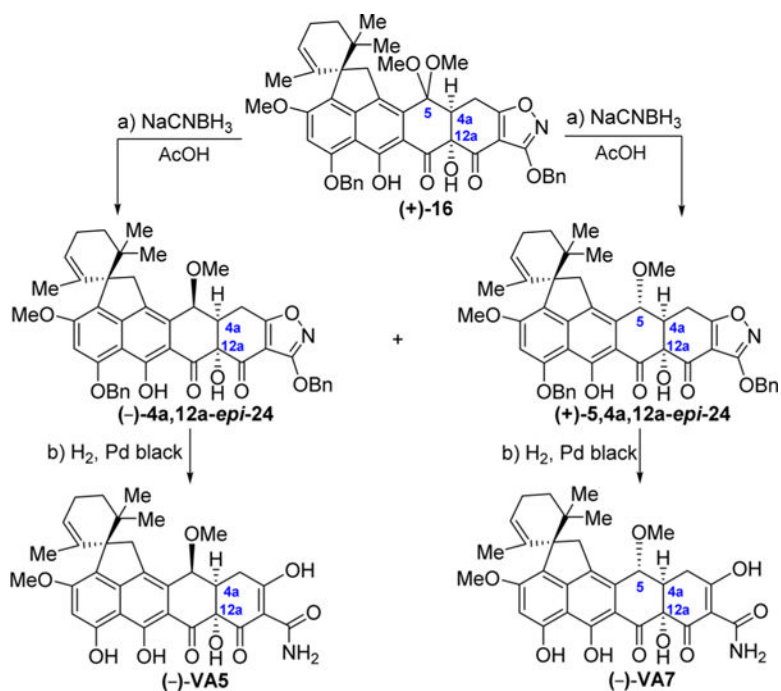
Scheme 3. Enantioselective Synthesis of the BCDEF Fragment (6R,15S)-4 of (+)-Viridicatumtoxin B and Its Absolute Configuration^a

^aReagents and conditions: (a) **7** (6.02 g, 16.0 mmol scale), **PTC17** (0.5 mol %), 40% aqueous Cs_2CO_3 , $(\text{CH}_2)_2\text{Cl}_2$, -30°C , 10 days, 73%, 95:5 dr; (b) hexanes, 91%, >99:1 dr; (c) $\text{BF}_3 \cdot \text{Et}_2\text{O}$ (0.05 equiv), CH_2Cl_2 , -78 to 0°C , 30 min, 74%, >99:1 er; (d) PIDA (1.2 equiv), $\text{MeOH}/\text{CH}_2\text{Cl}_2$ (1:1), 0°C , 30 min, 25°C , 30 min; (e) CSA (0.07 equiv), CH_2Cl_2 , 0°C , 5 min, 80% for two steps; (f) **10** (5.0 equiv), DMAP (10 equiv), Et_3N (30 equiv), CH_2Cl_2 , 25°C , 6 h, 95%. ^bTo avoid confusion, the numbering on **(6R,17S)-6**, **(6R,15S)-4** and **(+)-9** in this scheme and Figure 4 is based on the viridicatumtoxin numbering, as opposed to the carbon numbering of compound **(10R,14S)-6** (see Supporting Information), which is the same as **(6R,17S)-6**, the latter being designated using the anthrone numbering.



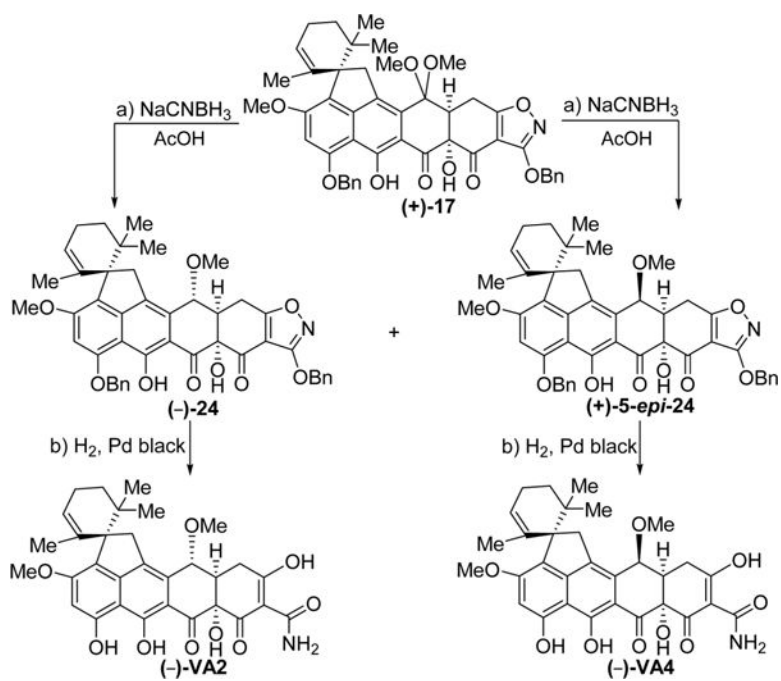
Scheme 4. Enantioselective Synthesis of Viridicatumtoxin B Analogues (+)-VA1 and (+)-VA3^a

^aReagents and conditions: (a) NaCNBH₃ (4.0 equiv), AcOH, 25 °C, 30 min, 48% for (+)-24, 32% for (-)-5-*epi*-24; (b) H₂, Pd black (4.1 equiv), THF/MeOH 1:1, 25 °C, 10 min, 95%.

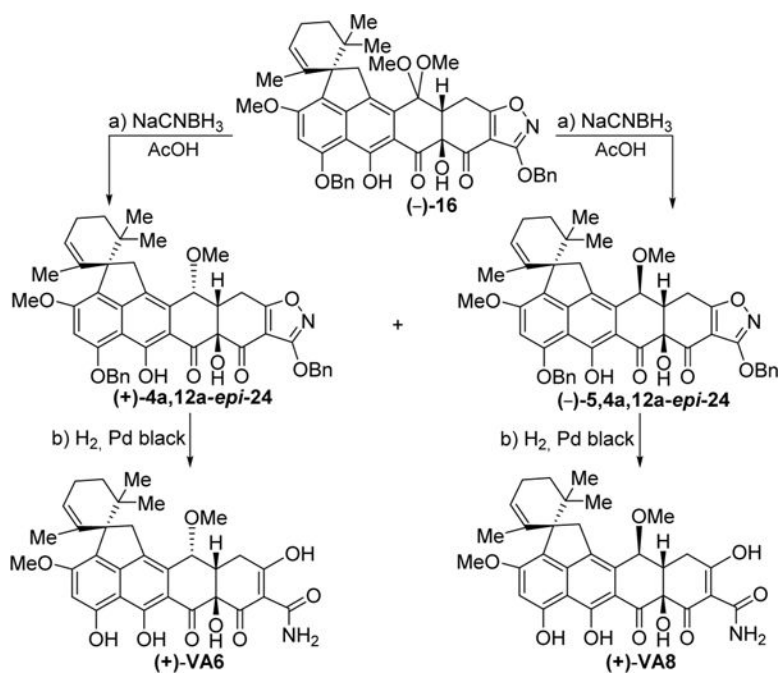


Scheme 5. Enantioselective Synthesis of Viridicatumtoxin B Analogues **{(-)-VA5 [(-)-4a,12a-epi-VA1], (-)-VA7 [(-)-5,4a,12a-epi-VA1]^a**

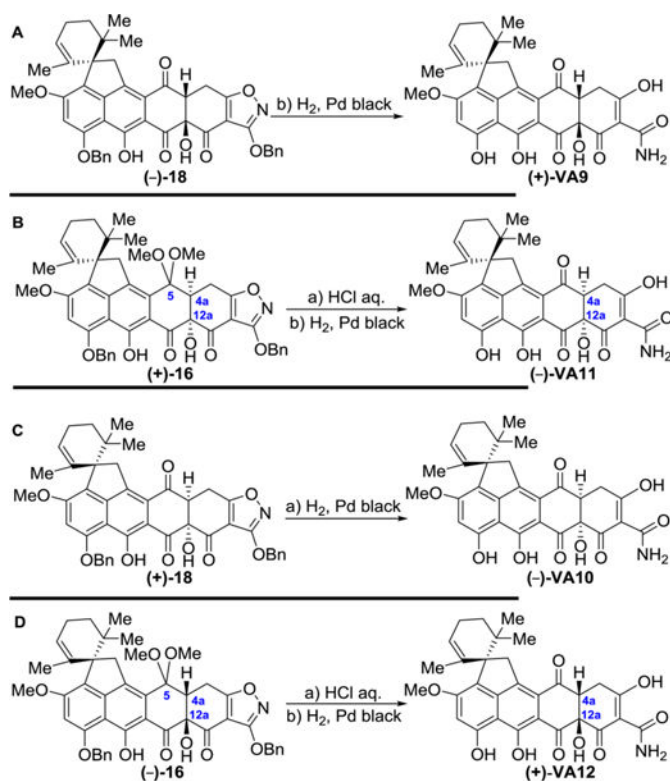
^aReagents and conditions: (a) NaCNBH₃ (4.0 equiv), AcOH, 25 °C, 30 min, 17% for **(-)-4a,12a-epi-24**, 51% for **(+)-5,4a,12a-epi-24**; (b) H₂, Pd black (4.1 equiv), THF/MeOH 1:1, 25 °C, 10 min, 95%.



Scheme 6. Enantioselective Synthesis of Viridicatumtoxin B Analogues (–)-VA2 and (–)-VA4^a
^aReagents and conditions: (a) NaCNBH₃ (4.0 equiv), AcOH, 25 °C, 30 min, 45% for (–)-24, 30% for (+)-5-*epi*-24; (b) H₂, Pd black (4.1 equiv), THF/MeOH 1:1, 25 °C, 10 min, 95%.



Scheme 7. Enantioselective Synthesis of Viridicatumtoxin B Analogues (+)-VA6 and (+)-VA8^a
^aReagents and conditions: (a) NaCNBH₃ (4.0 equiv), AcOH, 25 °C, 30 min, 16% for (+)-**4a**, **12a-epi-24**, 48% for (-)-**5,4a,12a-epi-24**; (b) H₂, Pd black (4.1 equiv), THF/MeOH 1:1, 25 °C, 10 min, 95%.



Scheme 8. Enantioselective Synthesis of Viridicatumtoxin B Analogues (+)-VA9, (-)-VA10, (-)-VA11, and (+)-VA12^a

^aReagents and conditions: Panel A: (a) H₂, Pd black (4.1 equiv), THF/MeOH 1:1, 25 °C, 10 min, 95%. Panel B: (a) 2 N aqueous HCl, THF, 25 °C, 5 h, quant.; (b) H₂, Pd black (4.1 equiv), THF/MeOH 1:1, 25 °C, 10 min, 95%. Panel C: (a) H₂, Pd black (4.1 equiv), THF/MeOH 1:1, 25 °C, 10 min, 95%. Panel D: (a) 2 N aqueous HCl, THF, 25 °C, 5 h, quant.; (b) H₂, Pd black (4.1 equiv), THF/MeOH 1:1, 25 °C, 10 min, 95%.

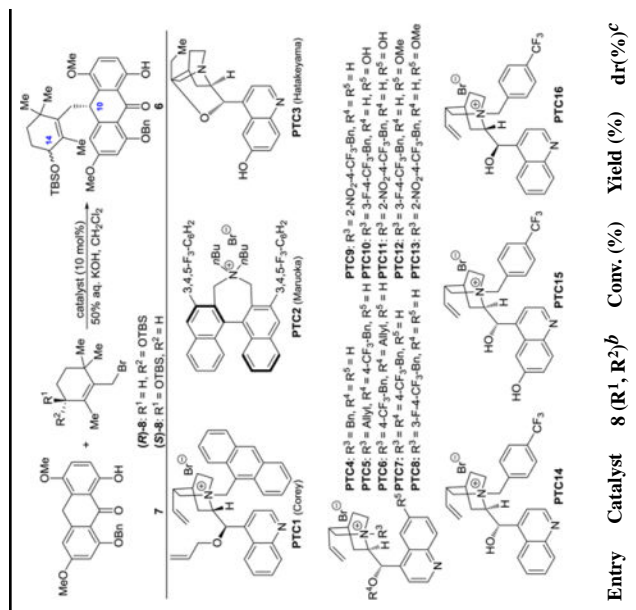
Catalyst Optimization of Alkylation of Anthrone 7 with Allylic Bromide 8 [(*R*) and/or (*S*)]^a

Entry	Catalyst	8 (<i>R</i> ¹ , <i>R</i> ²) ^b	Conv. (%)	Yield (%)	dr (%) ^c
1	PTC1	(<i>S</i>) and (<i>R</i>)	>99	78	62:38
2	PTC2	(<i>S</i>) and (<i>R</i>)	90	70	61:39
3	PTC3	(<i>S</i>) and (<i>R</i>)	>99	75	55:45
4	PTC4	(<i>S</i>) and (<i>R</i>)	>99	77	63:37
5	PTC5	(<i>S</i>) and (<i>R</i>)	>99	76	58:42
6	PTC6	(<i>S</i>) and (<i>R</i>)	>99	74	60:40
7	PTC7	(<i>S</i>) and (<i>R</i>)	>99	76	62:38
8	PTC8	(<i>S</i>) and (<i>R</i>)	>99	73	82:18
9	PTC9	(<i>S</i>) and (<i>R</i>)	80	70	83:17
10	PTC10	(<i>S</i>) and (<i>R</i>)	>99	72	80:20
11	PTC11	(<i>S</i>) and (<i>R</i>)	>99	70	79:21
12	PTC12	(<i>S</i>) and (<i>R</i>)	>99	72	58:42
13	PTC13	(<i>S</i>) and (<i>R</i>)	>99	75	64:36

Reaction scheme: Anthrone 7 + Allylic bromide 8 → Product 6. Conditions: catalyst (10 mol%), 50% aq. KOH, CH₂Cl₂.

PTC1 (Corey)
PTC2 (Manusaka)
PTC3 (Hatakeyama)

PTC4: R¹ = Bn, R² = H
PTC5: R¹ = Allyl, R² = H
PTC6: R¹ = 4-CF₃-Bn, R² = H
PTC7: R¹ = 4-CF₃-Bn, R² = H
PTC8: R¹ = 3-F-4-CF₃-Bn, R² = H
PTC9: R¹ = 2-NO₂-4-CF₃-Bn, R² = H
PTC10: R¹ = 3-F-4-CF₃-Bn, R² = OH
PTC11: R¹ = 2-NO₂-4-CF₃-Bn, R² = OH
PTC12: R¹ = 3-F-4-CF₃-Bn, R² = OMe
PTC13: R¹ = 2-NO₂-4-CF₃-Bn, R² = OMe
PTC14: R¹ = Bn, R² = H
PTC15: R¹ = 4-CF₃-Bn, R² = H
PTC16: R¹ = 3-F-4-CF₃-Bn, R² = H



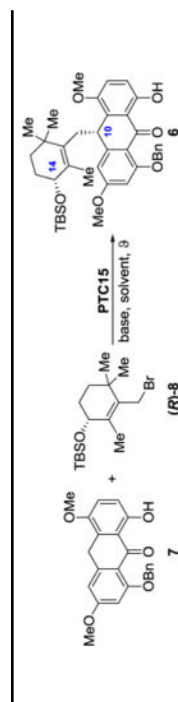
^aReaction conditions: anthrone **7** (0.10 mmol), allylic bromide **8** (0.11 mmol), PTC cat. (10 mol %), CH₂Cl₂ (0.9 mL), 50% aqueous KOH (0.3 mL), -78 to 0 °C, 8 h.

^b Allylic bromides (**R**)-**8** and (**S**)-**8** were prepared through a standard sequence⁴ involving CBS reduction¹⁹ of an intermediate enone as described in the Supporting Information.

^cThe diastereoisomeric ratio (dr) was determined by HPLC using a chiralPak AD-H column; the dr ratios for entries 1–15 were determined from the HPLC peak areas corresponding to (**10S**)-**6**: (**10R**)-**6** (see Supporting Information).

^dPTC16 is the pseudoenantiomer of PTC14.

Table 2

Optimization of Alkylation Conditions with PTC15^a


Entry	Base (aq. solution)	Solvent	ϕ (°C)	Time (h)	Cat. ^b (mol%)	Yield (%)	dr ^c
1	50% KOH	CH ₂ Cl ₂	0	8	10	77	89:11
2	50% NaOH	CH ₂ Cl ₂	0	8	10	77	89:11
3	50% Cs ₂ CO ₃	CH ₂ Cl ₂	0	8	10	77	91:9
4	50% K ₂ CO ₃	CH ₂ Cl ₂	0	8	10	75	91:9
5	40% Cs ₂ CO ₃	CH ₂ Cl ₂	0	8	10	75	92:8
6	30% Cs ₂ CO ₃	CH ₂ Cl ₂	0	8	10	73	91:9
7	40% Cs ₂ CO ₃	(CH ₂) ₂ Cl ₂	0	8	10	72	93:7
8	40% Cs ₂ CO ₃	CHCl ₃	0	8	10	60	85:15
9	40% Cs ₂ CO ₃	CCl ₄	0	8	10	50	81:19
10	40% Cs ₂ CO ₃	PhMe	0	8	10	78	84:16
11	40% Cs ₂ CO ₃	EtOAc	0	8	10	65	78:22
12	40% Cs ₂ CO ₃	(CH ₂) ₂ Cl ₂	-10	24	10	72	93:7
13	40% Cs ₂ CO ₃	(CH ₂) ₂ Cl ₂	-20	72	10	72	94:6
14	40% Cs ₂ CO ₃	(CH ₂) ₂ Cl ₂	-30	180	10	72	95:5
15	40% Cs ₂ CO ₃	(CH ₂) ₂ Cl ₂	-30	180	1	72	95:5
16 ^d	40% Cs ₂ CO ₃	(CH ₂) ₂ Cl ₂	-30	200	0.1	15	96:4

^a Reaction conditions: anthrone **7** (0.10 mmol), allylic bromide **(R)-8** (0.11 mmol), PTC15, solvent (0.9 mL), aqueous base solution (0.3 mL).^b Cat. = catalyst loading.

Author Manuscript

Author Manuscript

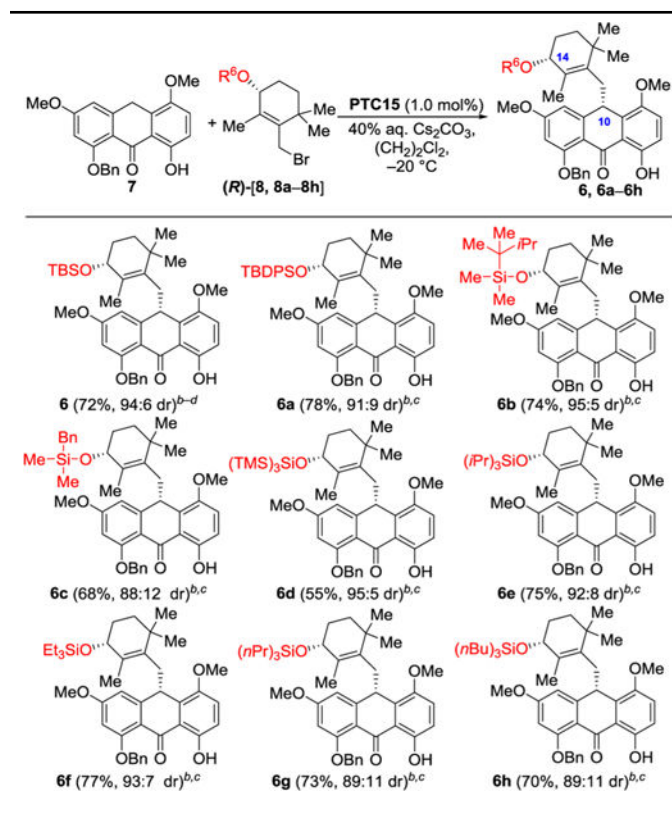
Author Manuscript

Author Manuscript

^cThe dr [(1*S*)-6-(**10R**)-9-(**9**)-(1*R*)] was determined by HPLC using a chiralPak AD-H column; see Supporting Information.

^dReaction was run on 5 mmol scale (anthrone). For further studies on possible C10 racemization of the alkylation product under basic conditions, see Supporting Information.

Table 3

Asymmetric Alkylation with Different Allylic Bromides^a

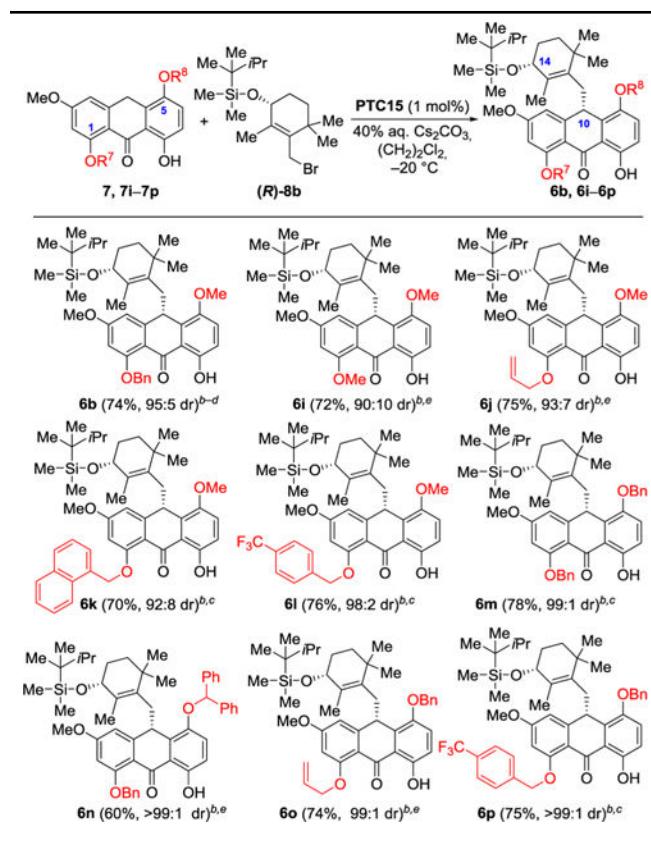
^aReaction conditions: anthrone **7** (0.10 mmol), allylic bromides **(R)-[8, 8a-8h]** (0.11 mmol), **PTC15** (1 mol %), $(\text{CH}_2)_2\text{Cl}_2$ (0.9 mL), 40% aqueous Cs_2CO_3 (0.3 mL), -20°C , 72 h.

^bIsolated yield.

^cThe dr [**10S**]:[**10R**] was determined by HPLC using a chiralPak AD-H column; see Supporting Information.

^dAs shown in Table 2, this reaction was repeated in this study as a further confirmation of its diastereoselectivity. TBS = *tert*-butyldimethylsilyl; TBDPS = *tert*-butyldiphenylsilyl.

Table 4

Asymmetric Alkylation with Different Anthrones^a

^aReaction conditions: anthrones **7**, **7i-7p** (0.10 mmol), **(R)-8b** (0.11 mmol), **PTC15** (1 mol %), $(\text{CH}_2)_2\text{Cl}_2$ (0.9 mL), 40% aqueous Cs_2CO_3 (0.3 mL), -20°C , 72 h.

^bIsolated yield.

^cThe dr ([**10S**):(**10R**)] was determined by HPLC using chiralPak AD-H column; see Supporting Information.

^dAs shown in Table 3, this reaction was repeated in this study as a further confirmation of its diastereoselectivity.

^eThe dr was determined by HPLC using chiralPak AD-H column after benzylation of the product; see Supporting Information.

Table 5

Minimum Inhibitory Concentration (MIC) Data of Compounds against Gram-Positive and Gram-Negative Bacteria and Comparison with Selected Literature Data

Entry	Gram-(+)						Gram-(-)			
	this study ^a			ref ¹			this study ^a		ref ¹	
	<i>E. faecalis</i> S613	<i>E. faecium</i> 105	MRSA 371	<i>E. faecalis</i> KCTC5191b	<i>E. faecium</i> KCTC3122b	MRSA CCARM3167b	<i>A. baumannii</i> AB210	<i>A. calcoaceticus</i> KCTC2357b	<i>E. coli</i> CCARM1356b	
CK1	8	8	1				4			
CK2	0.5	0.25	2				0.5			
(+)-1	2	2	4	2 ^c		0.5 ^c	64	1 ^c	>64 ^c	
(-)-1	4	4	8				64			
(+)-VA1	8	8	8				64			
(-)-VA2	16	16	32				64			
(+)-VA3	16	16	8				64			
(-)-VA4	8	16	64				64			
(-)-VA5	128	64	>128				64			
(+)-VA6	1	2	64				64			
(-)-VA7	4	8	8				64			
(+)-VA8	2	8	8				64			
(+)-VA9	0.5	2	2				64			
(-)-VA10	1	1	2				64			
(-)-VA11	1	0.5	2				64			
(+)-VA12	1	1	2				64			

^aMIC assays were run in triplicate; data are given in units of $\mu\text{g/mL}$.

^bTaken from ref¹ for comparison.

^cEnantiopure material [(+)-1] isolated from *Penicillium* sp. FR11 was used in ref¹.